Available online at www.sciencedirect.com
ScienceDirect
Journal of Solid State Chemistry 179 (2006) 3082–3086
JOURNAL OF SOLID STATE CHEMISTRY
www.elsevier.com/locate/jssc

$[C_6H_{21}N_4][Sb_9S_{14}O]$: Solvothermal synthesis, crystal structure and characterization of the first non-centrosymmetric open Sb–S–O framework containing the new $[SbS_2O]$ building unit

Ragnar Kiebach[a], Christian Näther[a], C. Peter Sebastian[b], Bernd D. Mosel[c], Rainer Pöttgen[b], Wolfgang Bensch[a,*]

[a]*Institut für Anorganische Chemie der Christian-Albrechts-Universität zu Kiel, Olshausenstraße 40, D-24098 Kiel, Germany*
[b]*Institut für Anorganische und Analytische Chemie and NRW Graduate School of Chemistry, Westfälische Wilhelms-Universität Münster, Corrensstrasse 30, 48149 Münster, Germany*
[c]*Institut für Physikalische Chemie, Westfälische Wilhelms Universität Münster, Corrensstrasse 30, 48149 Münster, Germany*

Received 24 February 2006; received in revised form 25 April 2006; accepted 28 May 2006
Available online 14 July 2006

Abstract

$[C_6H_{21}N_4][Sb_9S_{14}O]$ represents the first known oxo-thioantimonate with an organic ion acting as structure director. The compound crystallizes in the non-centrosymmetric space group $Cmc2_1$ with $a = 29.679(2)$, $b = 9.9798(6)$, $c = 11.7155(7)$ Å, $V = 3470.1(4)$ Å^3, $Z = 4$. The structure contains the hitherto unknown $[SbS_2O]$ unit as a structural motif. The $[SbS_3]$ trigonal pyramids and $[SbS_2O]$ units are joined to form a 10-membered ring with large pores having a diameter of 7.7 Å × 8.3 Å. The organic template molecule acts like a tetra-dentate ligand around the O atom of the $[SbS_2O]$ group. Depending on the value chosen for the Sb–S bond lengths, the material contains a 1-, 2- or 3-dimensional anion. The optical band gap of 2.03 eV demonstrates that the material is an optical semi-conductor. Upon heating, the compound decomposes in two steps yielding finally a mixture of Sb and Sb_2S_3. The ^{121}Sb Mössbauer spectrum shows a relative large line width in accordance with the superposition of the five signals.

Keywords: Oxo-thioantimonates; Hydrothermal synthesis; Mössbauer spectroscopy; Crystal structure

1. Introduction

The variety of microporous polyhedral framework solids has increased greatly in the past years [1]. In addition to the well-known microporous materials like aluminosilicates and aluminophosphates, the group of thioantimonates and oxo-thioantimonates blazed a trail to attractive candidates for applications. In the past years, remarkable properties like tunable optical band gaps, superconductivity or photoconductivity were discovered in the group of thioantimonates and/or antimony sulfides [2–9]. Another advantage of this group of compounds compared to aluminosilicates and aluminophosphates is the variety of different primary building units, their flexibility to adapt the requirements of the structure directors and the variable dimensionality [10–18]. The combination of properties of oxidic materials with that of sulfides will lead to a new class of materials with designable and interesting properties, making them highly attractive for applications like ion exchangers or catalysts. The so far unknown $[SbS_2O]$ unit found in $[C_6H_{21}N_4][Sb_9S_{14}O]$ (**1**) can be regarded as one "missing link" between oxide and sulfide materials and as a step toward a new class of materials. Here, we report the synthesis and characterization of the new oxo-thioantimonate $[C_6H_{21}N_4][Sb_9S_{14}O]$.

2. Experimental section

2.1. Synthesis

$[C_6H_{21}N_4][Sb_9S_{14}O]$ was synthesized under hydrothermal conditions using Sb_2O_3 (145 mg, 0.5 mmol) and

*Corresponding author. Fax: +49 431 880 1520.
E-mail address: wbensch@ac.uni-kiel.de (W. Bensch).

0022-4596/$ - see front matter © 2006 Elsevier Inc. All rights reserved.
doi:10.1016/j.jssc.2006.05.041

elemental S (96 mg, 3 mmol) in 4 mL of a 50% aqueous solution of *tren*. The mixture was heated to 150 °C for 7 days in Teflon-lined steel autoclaves (volume ca. 30 mL). The homogeneous product consisting of red crystals was filtered off, washed with distilled water, ethanol and acetone and was dried in air. The yield based on Sb is about 70%. Typical dimensions of the crystals are $0.7 \times 0.2 \times 0.2\,mm^3$. The compound is stable in air for several months.

2.2. X-ray crystallographic study

X-ray structure analysis and crystallographic data for **1**: The X-ray single-crystal data for **1** were collected using an Imaging Plate Diffraction System from STOE at 293 K. The intensities were corrected for Lorentz, polarization and absorption effects. Structure solution was performed using SHELXS-97 [19]. Refinement was done against F^2 using SHELXL-97 [20]. The non-hydrogen atoms were refined with anisotropic displacement parameters. The hydrogen atoms were positioned with idealized geometry and refined with isotropic displacement parameters using the riding model. Selected crystal data and details of the structure determination are listed in Table 1.

Crystallographic data (excluding structure factors) for the structure reported in this paper have been deposited with the Cambridge Crystallographic Data Centre as supplementary Publication No. CCDC-275176. Copies of the data can be given free of charge on application to CCDC, 12 Union Road, Cambridge CB21EZ, UK (fax: +44 1223 336 033; E-mail: deposit@ccdc.cam.ac.uk).

2.3. Thermal investigation

Differential thermoanalysis and thermogravimetry (DTA–TG) were performed using a Netzsch STA 429 DTA–TG device. The sample was heated in Al_2O_3 crucibles at a rate of $4\,K\,min^{-1}$ to 600 °C under a flow of argon of $100\,mL\,min^{-1}$.

2.4. Powder diffraction

X-ray powder diffraction experiments were performed using a STOE STADI P transmission powder diffractometer with a position sensitive detector and Cu-K_α radiation ($\lambda = 1.540598$ Å).

2.5. UV/Vis spectroscopy

UV/Vis spectroscopic investigations were conducted at room temperature using a UV–VIS–NIR two-channel spectrometer Cary 5 from Varian Techtron Pty., Darmstadt. The optical properties of the compound was investigated by studying the UV/Vis reflectance spectrum of the powdered sample. The absorption data were calculated using the Kubelka–Munk relation for diffuse

Table 1
Crystal data and selected results of the structure refinement for $[C_6H_{21}N_4][Sb_9S_{14}O]$

Empirical formula	$C_6H_{21}N_4OS_{14}Sb_9$
Crystal color	Red
Crystal habit	Polyhedra
Molecular mass (g/mol)	1709.86
Crystal system	Orthorhombic
Space group	$Cmc2_1$
a (Å)	29.679(2)
b (Å)	9.9798(6)
c (Å)	11.7155(7)
V (Å^3)	3470.1(4)
Z	4
T (K)	293
λ(Mo-K_α) (Å)	0.71073
$d_{calcd.}$ (mg cm^{-3})	3.273
μ(Mo-K_α) (mm^{-1})	7.749
F(000)	3104
Reflections collected	18706
Independent reflections	4217
Reflections with $F_o > 4\sigma(F_o)$	3718
wR_2 for all reflections[a]	0.0897
R_1 for reflections with $F_o > 4\sigma$ (Fo)[b]	0.0346
Goodness of fit	1.028
Flack x-parameter	−0.05(4)
Largest diff. peak/hole (e Å^{-3})	2.34/−1.42

[a] $wR_2 = [\Sigma[w(F_o^2 - F_c^2)^2]/\Sigma[w(F_o^2)^2]]^{1/2}$.
[b] $R_1 = \Sigma||F_o| - |F_c||/\Sigma|F_o|$.

Table 2
Selected bond lengths (Å) and angles (deg) for $[C_6H_{21}N_4][Sb_9S_{14}O]$

Sb(1)–S(4)	2.407(2)	Sb(1)–S(1)	2.477(3)
Sb(1)–S(3)	2.493(2)	Sb(2)–S(2)	2.474(2)
Sb(2)–S(1)	2.487(2)	Sb(2)–S(5)	2.492(2)
Sb(3)–S(2)	2.464(2)	Sb(3)–S(3)	2.475(2)
Sb(3)–S(6)	2.530(2)	Sb(4)–S(5)	2.426(3)
Sb(4)–S(6)	2.450(2)	Sb(4)–S(7)	2.488(2)
Sb(5)–O(1)	1.956(10)	Sb(5)–S(7)	2.437(3)
Sb(5)–S(7)	2.437(3)	S(5)–Sb(4)	2.426(3)
N(1)–C(1)	1.499(18)	C(1)–C(2)	1.485(16)
C(2)–N(2)	1.492(14)	N(2)–C(3)	1.50(2)
C(3)–C(4)	1.41(3)	C(4)–N(3)	1.37(3)
S(4)–Sb(1)–S(1)	95.94(8)	S(4)–Sb(1)–S(3)	95.01(7)
S(1)–Sb(1)–S(3)	95.71(8)	S(2)–Sb(2)–S(1)	101.05(8)
S(2)–Sb(2)–S(5)	83.98(8)	S(1)–Sb(2)–S(5)	89.57(9)
S(2)–Sb(3)–S(3)	99.19(8)	S(2)–Sb(3)–S(6)	83.92(8)
S(3)–Sb(3)–S(6)	89.23(8)	S(5)–Sb(4)–S(6)	96.63(9)
S(5)–Sb(4)–S(7)	95.40(10)	S(6)–Sb(4)–S(7)	93.31(8)
O(1)–Sb(5)–S(7)	96.5(3)	O(1)–Sb(5)–S(7)	96.5(3)
S(7)–Sb(5)–S(7)	86.84(12)	Sb(1)–S(1)–Sb(2)	98.86(8)
Sb(3)–S(2)–Sb(2)	105.48(8)	Sb(3)–S(3)–Sb(1)	98.35(8)
Sb(4)–S(5)–Sb(2)	101.96(9)	Sb(4)–S(6)–Sb(3)	100.91(8)
Sb(5)–S(7)–Sb(4)	109.60(11)	C(2)–C(1)–N(1)	111.4(10)
C(1)–C(2)–N(2)	111.3(10)	C(2)–N(2)–C(2)	108.5(12)
C(2)–N(2)–C(3)	112.3(8)	C(2)–N(2)–C(3)	112.3(8)
C(4)–C(3)–N(2)	114.4(16)	N(3)–C(4)–C(3)	130.9(18)

Estimated standard deviations are given in parentheses.

reflectance data. $BaSO_4$ powder was used as reference material.

2.6. Mössbauer spectroscopy

A $Ba^{121m}SnO_3$ source was used for the Mössbauer spectroscopic experiments. The measurements were carried out in a helium bath cryostat, at 20 K for $[C_6H_{21}N_4][Sb_9S_{14}O]$, and at room temperature for Sb_2S_3 and Sb_2S_2O. The temperature was controlled by a resistance thermometer (± 0.5 K accuracy). The Mössbauer source was kept at room temperature. The samples were enclosed in small PVC containers at a thickness corresponding to approximately 10 mg Sb/cm^2.

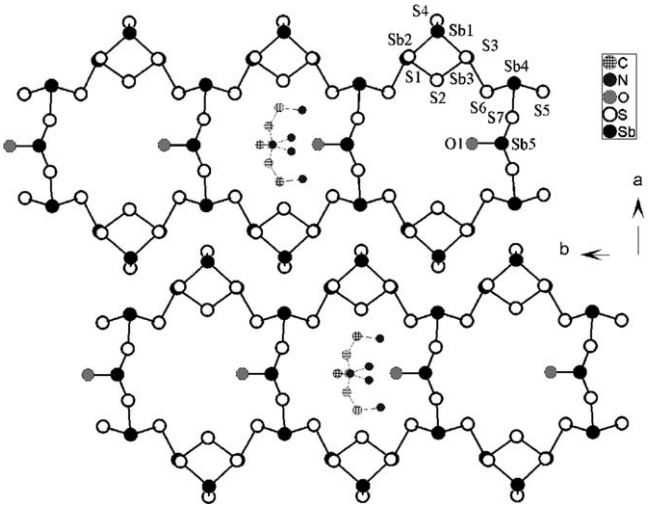

Fig. 1. The $[Sb_9S_{14}O]^{3-}$ chains directed along the *b*-axis. Cations are only shown in the middle. Hydrogen atoms omitted for clarity.

3. Results and discussion

3.1. Crystal structure

The compound was prepared under solvothermal conditions using tris(2-aminoethyl)amine (*tren*) as solvent and as structure directing molecule. It crystallizes in the non-centrosymmetric orthorhombic space group $Cmc2_1$ (see Section 2) and consists of infinite $[Sb_9S_{14}O]^{3-}$ chains with protonated amine molecules as counter ions. The anion is constructed by interconnection of four unique $[SbS_3]$ and one unique $[SbS_2O]$ group sharing common corners. The $[SbS_2O]$ unit was never observed before in oxosulfide minerals [21–24] or in synthetic oxo-thioantimonates. The $[SbS_3]$ and the $[SbS_2O]$ units have typical trigonal pyramidal geometry with Sb–S bond lengths between 2.407(2) and 2.530(2) Å and corresponding S–Sb–S angles between 83.92(8)° and 101.05(8)° (Table 2). The Sb–O bond in $[SbS_2O]$ of 1.956(10) Å is significantly shorter than the Sb–S bonds. The bond lengths and angles are comparable to those found in other thioantimonates and in oxo-thioantimonates [2–18,21–24]. Eight $[SbS_3]$ trigonal pyramids and two $[SbS_2O]$ units are joined to form a 10-membered ring in which one *tren* molecule is located. The diameter of the pore is 7.66 Å × 8.27 Å measured from coordinate to coordinate (Fig. 1). The triply protonated *tren* molecule acts like a tetra-dentate ligand around the oxygen atom of the $[SbS_2O]$ group (Fig. 1), reflecting the structure-directing effect. The 1-D $[Sb_9S_{14}O]^{3-}$ chain is directed along the *b*-axis (Fig. 1) and is constructed by condensation of the 10-membered rings mentioned above. The separation between the chains is approximately 3.25 Å and taking the longer Sb–S distances into account, layers are formed. The shortest interlayer distance amounts to 3.47 Å. A three-dimensional arrangement is achieved by six N–H · S and two N–H · O hydrogen bonds. If the long Sb–S separations up to 3.7 Å are treated as weak interactions, the network is three-dimensional (Fig. 2). The bond valence sum was calculated [25] for the $[SbS_2O]$ unit yielding 3.25

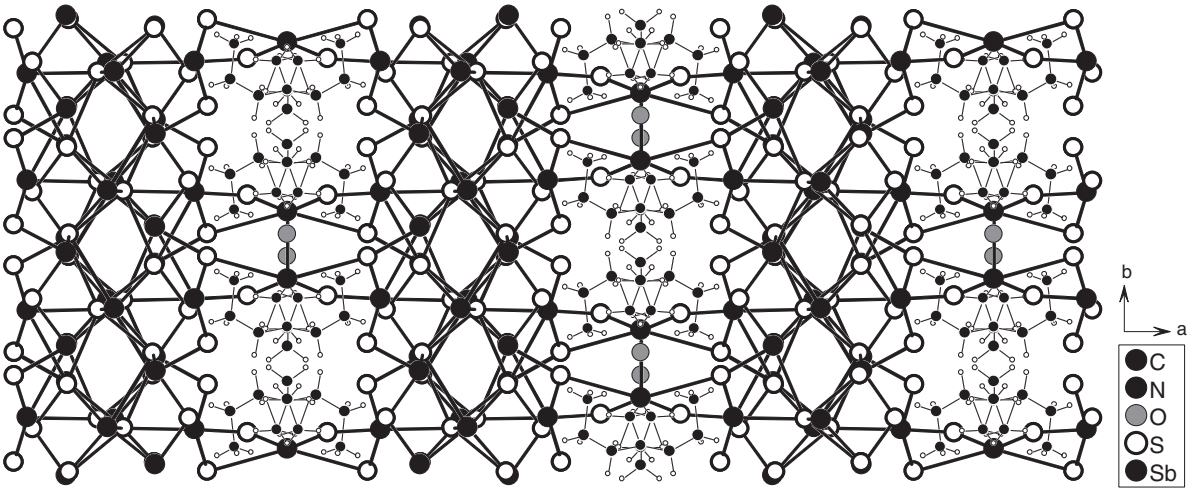

Fig. 2. Crystal structure of $[C_6H_{21}N_4][Sb_9S_{14}O]$ with view along the *c*-axis, long Sb–S bonds up to 3.7 Å are considered.

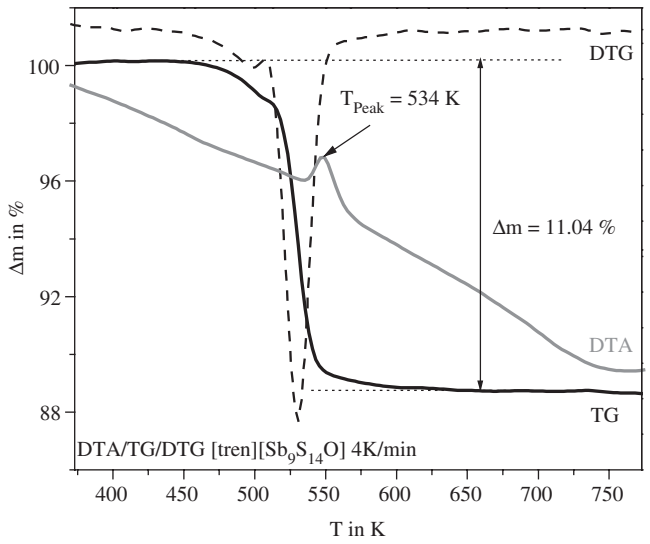

Fig. 3. DTA, TG and DTG curves for $[C_6H_{21}N_4][Sb_9S_{14}O]$, given are the mass loss in % and the peak temperature T_P in °C.

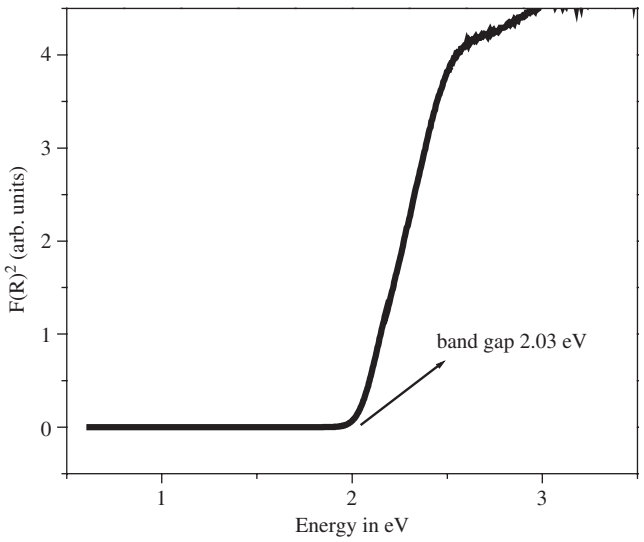

Fig. 4. UV/Vis spectrum of $[C_6H_{21}N_4][Sb_9S_{14}O]$.

for the Sb atom. Replacing the O atom in this group by a S atom gives the not realistic value of 6.26.

3.2. Thermal investigations

The thermal stability was investigated using simultaneous DTA and TG under an argon atmosphere in the range from 298 to 773 K (Fig. 3). The material decomposes in two not well-resolved steps with a total mass loss of 11.04% at $T_{onset} = 493$ K. The decomposition reaction is accompanied by an endothermic event at $T_P = 534$ K (T_P = peak temperature). In the gray residue, only small amounts of organic components were found (C: 0.254%; H: 0.022%; N: 0.133%; $CHN_{sum} = 0.406\%$). The experimental mass loss of 11.04% is in agreement with that calculated for the removal of the organic cations ($\Delta m_{theo} = 9.67\%$), the difference of 1.37% is caused by the emission of H_2S, which was detected in mass spectra. In the X-ray powder pattern of the decomposition products crystalline Sb and Sb_2S_3 could be identified.

3.3. Optical properties

The optical band gap was calculated from UV/Vis data after the method of Kubelka and Munk. An absorption

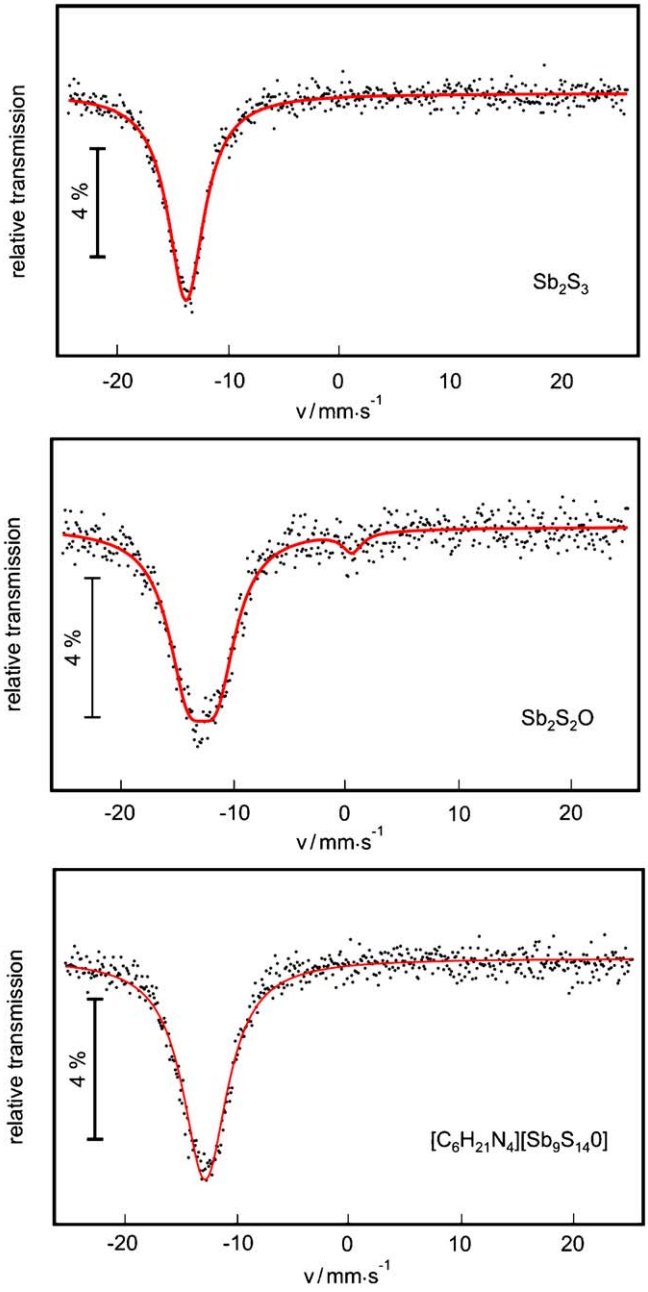

Fig. 5. ^{121}Sb Mössbauer spectra of Sb_2S_3 (top), Sb_2S_2O (middle), $[C_6H_{21}N_4][Sb_9S_{14}O]$ (bottom).

Table 3
^{121}Sb Mössbauer spectra of Sb_2S_3, Sb_2S_2O (room temperature data) and $[C_6H_{21}N_4][Sb_9S_{14}O]$ (20 K data)

Compound	δ_1 (mm/s)	ΔEQ (mm/s)	Γ_1 (mm/s)	δ_2 (mm/s)	Γ_2 (mm/s)	χ^2
Sb_2S_3	−14.44(2)	—	3.92(6)	—	—	1.13(2)
Sb_2S_2O	−12.64(3)	−2.53(9)	4.24(1)	0.63(2)	2.03(5)	1.05(1)
$[C_6H_{21}N_4][Sb_9S_{14}O]$	−12.66(3)	—	4.76(8)	—	—	1.08(1)

δ = isomer shift, ΔEQ = electric quadrupole interaction parameter, Γ = experimental line width, χ^2 = goodness of fit.

edge is observed at 2.03 eV (600 nm) (Fig. 4), corresponding to the red color of $[C_6H_{21}N_4][Sb_9S_{14}O]$ and the material is an optical semi-conductor. In combination with the non-centrosymmetric space group $[C_6H_{21}N_4][Sb_9S_{14}O]$ is a potential candidate for NLO effects.

3.4. Mössbauer spectroscopy

To support the results from single-crystal structure refinement, ^{121}Sb Mössbauer spectroscopic experiments were performed. As references, Sb_2S_3 and Sb_2S_2O (Kermesite, contains $[SbS_3]$ and $[SbSO_2]$ units) were measured. The ^{121}Sb Mössbauer spectra of Sb_2S_3, Sb_2S_2O (room temperature data) and of $[C_6H_{21}N_4][Sb_9S_{14}O]$ (20 K data) are presented in Fig. 5. The fitting parameters are listed in Table 1. The spectrum of Sb_2S_3 shows a single signal at an isomer shift of −14.44(2) mm/s, in good agreement with the literature [26]. Kermesite, Sb_2S_2O, shows a smaller isomer shift of −12.64(3) mm/s, indicating a smaller *s*-electron density at the antimony nucleus. A small Sb(V) impurity was included in the fit of the spectrum. Due to the low space group symmetry (triclinic) [27], a small quadrupole splitting occurs for the Sb(III) site (Table 3).

Although the $[C_6H_{21}N_4][Sb_9S_{14}O]$ structure has five crystallographically independent Sb(III) sites, the ^{121}Sb spectrum can be fitted with a single signal at an isomer shift of −12.66(3) mm/s. The experimentally observed line width of 4.76(8) mm/s is somewhat enhanced and accounts for the superposition of the five signals. Unfortunately, it was not possible to fit the $[SbS_2O]$ unit as an independent site in the ^{121}Sb Mössbauer spectrum.

Acknowledgment

Financial support by the State of Schleswig-Holstein and the Deutsche Forschungsgemeinschaft is gratefully acknowledged.

References

[1] A.K. Cheetham, G. Férey, T. Loiseau, Angew. Chem. Int. Ed. 38 (1999) 3268–3292.
[2] M. Schaefer, R. Stähler, R. Kiebach, C. Näther, W. Bensch, Z. Anorg. Allg. Chem. 630 (2004) 1816–1822.
[3] C.-S. Lee, A. Safa-Sefat, J.E. Greedan, H. Kleinke, Chem. Mater. 15 (2003) 780–786.
[4] F. Starrost, E.E. Krasovskii, W. Schattke, U. Simon, X. Wang, F. Liebau, Phys. Rev. Lett. 80 (1998) 3316–3319.
[5] X. Wang, F. Liebau, Eur. J. Solid State Inorg. Chem. 15 (1998) 27–37.
[6] F. Liebau, Z. Kristallogr. 215 (2000) 381–383.
[7] U. Simon, V. Gasparian, Phys. Stat. Sol. B 218 (2000) 151–154.
[8] U. Simon, F. Schüth, S. Schunk, X. Wang, F. Liebau, Angew. Chem. Int. Ed. 36 (1997) 1121–1124.
[9] F. Starrost, E.E. Krasovskii, W. Schattke, J. Jockel, U. Simon, R. Adelung, L. Kipp, Phys. Rev. B 61 (2000) 15697–15706.
[10] R. Stähler, C. Näther, W. Bensch, J. Solid State Chem. 174 (2003) 264–275.
[11] V. Spetzler, R. Kiebach, C. Näther, W. Bensch, Z. Anorg. Allg. Chem. 630 (2004) 2398–2404.
[12] R. Kiebach, C. Näther, W. Bensch, Z. Naturforsch. 59b (2004) 1314–1319.
[13] R. Kiebach, C. Näther, W. Bensch, R.-D. Hoffmann, R. Pöttgen, Z. Anorg. Allg. Chem. 629 (2003) 532–538.
[14] P. Vaqueiro, A.M. Chippindale, A.V. Powell, Inorg. Chem. 43 (2004) 7963–7965.
[15] A.V. Powell, S. Boissiere, A.M. Chippindale, Chem. Mater. 12 (2000) 182–187.
[16] A.V. Powell, R. Paniagua, P. Vaqueiro, A.M. Chippindale, Chem. Mater. 12 (2002) 1220–1224.
[17] J.B. Parise, Y. Ko, Chem. Mater. 4 (1992) 1446–1450.
[18] G. Dittmar, H. Schäfer, Z. Anorg. Allg. Chem. 437 (1977) 183–187.
[19] G.M. Sheldrick, SHELXS-97, Program for Crystal Structure Determination, University of Göttingen, Germany, 1997.
[20] G.M. Sheldrick, SHELXL-97, Program for the Refinement of Crystal Structures, University of Göttingen, Germany, 1997.
[21] E.M. Baumgardt, V. Kupcik, J. Cryst. Growth 37 (3) (1977) 346–348.
[22] V. Kupcik, Naturwissenschaften 54 (5) (1967) 114.
[23] A. Meerschaut, P. Palvadeau, Y. Molëo, P. Orlandi, Eur. J. Mineral. 13 (2001) 779–790.
[24] Y. Molëo, A. Meerschaut, P. Orlandi, P. Palvadeau, Eur. J. Mineral 12 (2000) 835–846.
[25] I.D. Brown, D. Altermatt, Acta Crystallogr. B 41 (1985) 244–247.
[26] P.E. Lippens, Solid State Commun. 113 (2000) 399–403.
[27] P. Bonazzi, S. Menchetti, C. Sabelli, Neues Jahrbuch für Mineralogie, Neues Jahrb. Mineral. Monatsh. (1987) 557–565.